Paper No.
02238

CORROSION 2002

CO_2 CORROSION MECHANISTIC MODELING AND PREDICTION IN HORIZONTAL SLUG FLOW

Hongwei Wang*, Ji-Yong Cai♣, William Paul Jepson
NSF, I/UCRC Corrosion in Multiphase System Center
Institute for Corrosion and Multiphase Technology
Ohio University
340 ½ West State Street, Athens, OH 45701, USA

ABSTRACT

This paper presents a CO_2 corrosion mechanistic model specifically developed for the horizontal multiphase slug flow. It covers electrochemical reactions at the steel surface, transport of reactive species between the metal surface and the bulk, and the chemistry in the bulk solution. The special mass transfer correlations in slug flow were applied in this model. The model can predict the corrosion rate in horizontal slug flow. Comparison with laboratory experimental corrosion results revealed that it could help the understanding of the internal corrosion of horizontal pipeline under slug flow condition. Furthermore, this model shows that the Froude number and the slug frequency are two important factors influencing the internal corrosion rates under multiphase slug flow. This provides an insight for the pipeline design and production under multiphase slug flow.

INTRODUCTION

Internal corrosion of carbon steel pipelines is a common problem in oil and gas production facilities, which are designed for long-time operation. This problem has caused the consideration of many corrosion control programs and research in various oil fields around the world. One of the most important research is the numerous prediction modeling for CO_2 corrosion of carbon steel. Nesic et al. gave a thorough review of CO_2 corrosion modeling in 1997.[1]

The use of multiphase pipelines is now very common in the production of oil and gas. The

---

* Current address: Dept. of Material Science & Engineering, University of Virginia, Charlottesville, VA 22903, USA
♣ Current address: Dept. of Chemical & Materials Engineering, University of Alberta, Edmonton, AB T5K 1V5, Canada

oil/water/gas mixture from several wells is often transported several tens of kilometers to a platform or central gathering station where separation takes place. In these multiphase flow lines, several flow regimes exist which include stratified, slug, and annual flow as shown in Figure 1. The earlier CO_2 corrosion modeling did not consider much on the influence of multiphase flow. In recent years, bringing the influence of multiphase flow into the corrosion model becomes a trend as shown in Table 1. It shows the major commercial corrosion prediction models or softwares currently used in the oil and gas industry.[2-16] Most of models can only be used for corrosion in turbulent flow or gas well. Several models have been extended from single phase flow to multiphase flow with some specific assumptions.[5, 8, 10, 11, 13-15]

At high production rates, the pipeline operates under slug flow conditions. A typical slug is depicted in Figure 2(a), including slug mixing zone, slug body, slug tail, and slug film four regions. The high turbulence in slug flow causes a high corrosion rate of carbon steel, which was first reported by Green et al. in 1990.[17] Therefore, in recent years, the effects of multiphase slug flow on CO_2 corrosion have been studied extensively in large flow loops, e.g. 4 inch I.D. pipeline, via advanced hydrodynamics measurement techniques, electrochemical corrosion test methods, [18, 19] and corrosion modeling.[14]

Very few models specifically investigated the influence of multiphase slug flow on the corrosion. Two models, Pots and IFE Model have given some considerations of slug flow. Both models simplified the slug flow into two regions only: a slug film zone and a slug mixing zone as shown in Figure 2. Corrosion rates were then calculated separately for film and slug zones. The film zone was considered like the separated flow. For the slug zone, the relevant flow velocity is the mixture velocity, the sum of the superficial liquid velocity and the superficial gas velocity. The hydraulic diameter equals the pipe diameter. The overall corrosion rate was calculated by averaging the corrosion rates in the two zones. It can be found that both models have ignored the highly turbulent flow conditions that exist in the slug mixing zone. However, it is this unique turbulence in slug flow that causes the enhanced corrosion rates.[20-22] Therefore, the above simplification is not effective since these models usually underestmiates the corrosion rates in slug flow.

The Ohio model has been developed in the past several years. It combined the fluid dynamic models and the corrosion prediction models. The fluid dynamic models included flow regime prediction, water/oil flow, and slug flow tracking. The corrosion prediction models included a specific corrosion mechanistic model for turbulent flow and water/oil flow,[13] and a semi-emipirical corrosion model for multiphase slug flow.[14]

Gunaltun proposed that it is impossible to use the same model or correlation for the prediction of the corrosion for both gas lines and oil lines or for wells and flow lines due to the fact that corrosive mediums and flow regimes are quite different.[6] For each case, parameters to be used need to be identified and calculated separately for the specified conditions. The special hydrodynamic characteristics studies[23-28] and the recent studies[29-34] of the effects of gas bubbles on mass transfer and shear stress indicated that it is not only necessary but also ready to develop a corrosion mechanistic model specifically for slug flow.

This paper aims to develop a CO_2 mechanistic corrosion model in slug flow, taking into account the special mass transfer in slug flow. These well established theoretical paths developed or used by Dayanan et al. (1996), Pots (1995), Zhang et al. (1998) were adopted into this study. The experimental corrosion data in slug flow produced in the Institute of Corrosion and Multiphase Technology were used to validate this corrosion mechanistic model developed for slug flow.

CO_2 MECHANISTIC MODELING IN HORIZONTAL SLUG FLOW

Simplified CO_2 Corrosion Mechanistic Model without Corrosion Product Layer

When the reactants reach the metal surface, various electrochemical reactions take place between the metal surface and the species. This model assumes that only the following reactions take place at the surface. This assumption is practical especially in the gas-condensed pipeline under slug flow condition where pH is usually low.

Cathodic reaction:

$$2H^+ + 2e^- \rightarrow H_2 \quad (1)$$

Anodic reaction:

$$Fe \rightarrow Fe^{2+} + 2e^- \quad (2)$$

The current densities i_a, i_c due to the above electrochemical reactions are given by the Butler-Volmer equation, and can be written as:

$$i_a = 2FK_{e,Fe^{2+}}[Fe^{2+}]_s \exp[\frac{2(1-\alpha)F(E_{corr} - E_{Fe^{2+}})}{RT}] \quad (3)$$

$$i_c = 2FK_{e,H^+}[H^+]_s \exp[\frac{-2\alpha F(E_{corr} - E_{H^+})}{RT}] \quad (4)$$

Where,

i_a = anodic current density (A/m^2)
i_c = cathodic current density (A/m^2)
$[Fe^{2+}]_s$ = surface concentration of Fe^{2+} (mol/m^3)
$[H^+]_s$ = surface concentration of H^+ (mol/m^3)
E_{corr} = corrosion potential (V)
α = transfer coefficient (=0.5 for most cases)
F = Faraday's constant (=96500 C/mol)
R = universal gas constant (=8.314 J/mol-K)
T = temperature (K)
$E_{Fe^{2+}}$ = potential for the anodic reaction (V)
$E_{H^{2+}}$ = potential for the cathodic reaction (V)
$K_{e,Fe^{2+}}$ = rate constants for the anodic reaction (m/s)
K_{e,H^+} = rate constants for the cathodic reaction (m/s)

The values of the rate constants are not available readily in the literature at all temperatures and for all material types. From Tanaka and Tamamushi,[35] the rate constant increases with temperature and is about one order magnitude higher for every 20 °C. In this study, the values for the rate constants (K_{e,H^+}, $K_{e,Fe^{2+}}$) are 2×10^{-3} and 2.59 cm/s, respectively, for hydrogen ion reduction and iron dissolution reactions at 80 °C, which are suggested by Dayalan et al. (1995). At 60 °C, the values for the rate

constants ($K_{e,H^+}, K_{e,Fe^{2+}}$) are 2×10^{-4} and 0.259 cm/s, respectively, while they are 2×10^{-5} and 0.0259 cm/s respectively at 40 °C.

The equilibrium potentials E_{H^+} and $E_{Fe^{2+}}$ are given by the Nernst equations:

$$E_{H^+} = E^0{}_{H^+} + \frac{RT}{nF} \ln \frac{[H^+]_s{}^2}{[H_2]} \tag{5}$$

$$E_{Fe^{2+}} = E^0{}_{Fe^{2+}} + \frac{RT}{nF} \ln [Fe^{2+}]_s \tag{6}$$

Where,

H_2 = surface concentration of H_2 (mol/m^3)

$E^0{}_{H^+}$ = standard potential for the cathodic reactions (V)

$E^0{}_{Fe^{2+}}$ = standard potential for the anodic reactions (V)

Assuming steady state, the sum of the currents due to the cathodic reactions should be equal to the sum of the currents due to the anodic reactions, which in turn is equal to the corrosion current.

$$i_c = i_a = i_{corr} \tag{7}$$

For iron, corrosion rate is calculated by:

$$CR = \frac{i_a}{2F} \frac{M_{Fe}}{\rho_{Fe}} \times 3600 \times 24 \times 365 = 1.16 i_a \tag{8}$$

Where,

CR = corrosion rate (mm/year)

i_a = anodic current density (A/m^2)

F = Faraday's constant (=96500 C/mol)

M_{Fe} = iron molecular weight (=55.85 kg/kmol)

ρ_{Fe} = iron mass density (=7800kg/m^3)

Under steady state conditions it is assumed the sum of the mass transfer rates of the reactant are equal to the sum of the electrochemical reaction rates. Hence we can write,

$$2FK_{mt,Fe^{2+}}([Fe^{2+}]_s - [Fe^{2+}]_b) = i_a \tag{9}$$

$$FK_{mt,H^+}([H^+]_b - [H^+]_s) = i_c \tag{10}$$

The subscripts s and b represents the surface and bulk, respectively. The three unknowns are surface concentrations of Fe^{2+} and H^+, along with the corrosion potential $E_{corr.}$ Three Equations 7, 9, and 10 are used to solve these three unknowns; finally, Equation 8 can determine the corrosion rate.

Numerical Solution of Corrosion Rate

These three unknowns, which are surface concentration of ferrous ion, surface concentration of hydrogen ion, and corrosion potential, can be solved by a set of three nonlinear equations. These three nonlinear equations were linearized and were solved by using the Newton-Raphson method as described below. In this method these three equations were written in the form of $F_i(x_j)=0$, where x_j is the variable vector and F_i is the residual vector as shown below with i and j ranging from 1 to 3. Equations 3, 4, 7, 9, and 10 after rearranging gives,

$$F_1 = K_{mt,Fe^{2+}}(x_1 - [Fe^{2+}]_b) - K_{e,Fe^{2+}} x_1 \exp\left[\frac{2(1-\alpha)F\left(x_3 - E^0_{Fe^{2+}} - \frac{RT}{2F}\ln(x_1)\right)}{RT}\right] = 0 \quad (11)$$

$$F_2 = K_{mt,H^+}([H^+]_b - x_2) - 2K_{e,H^+} x_2 \exp\left[\frac{-2\alpha F\left(x_3 - E^0_{H^+} - \frac{RT}{2F}\ln\left(\frac{x_2^2}{H_2}\right)\right)}{RT}\right] = 0 \quad (12)$$

$$F_3 = K_{e,H^+} x_2 \exp\left[\frac{-2\alpha F\left(x_3 - E^0_{H^+} - \frac{RT}{2F}\ln\left(\frac{x_1^2}{H_{2\,1}}\right)\right)}{RT}\right] - K_{e,Fe^{2+}} x_1 \exp\left[\frac{2(1-\alpha)F\left(x_3 - E^0_{Fe^{2+}} - \frac{RT}{2F}\ln(x_1)\right)}{RT}\right] = 0 \quad (13)$$

Where,

x_1 = surface concentration of Fe^{2+} (mol/m^3)
x_2 = surface concentration of H^+ (mol/m^3)
x_3 = corrosion potential (V)
α = transfer coefficient (=0.5 for most cases)
F = Faraday's constant (=96500 C/mol)
R = universal gas constant (=8.314 J/mol-K)
T = temperature (K)
$K_{mt,Fe^{2+}}$ = mass transfer coefficient for Fe^{2+} (m/s)
K_{mt,H^+} = mass transfer coefficient for H^+ (m/s)
K_{e,H^+} = rate constant for cathodic reaction (m/s)
$K_{e,Fe^{2+}}$ = rate constant for anodic reaction (m/s)
H_2 = surface concentration of H_2 gas (mol/m^3)
$E^0_{H^+}$ = standard potential for the cathodic reaction (V)
$E^0_{Fe^{2+}}$ = standard potential for the anodic reaction (V)
$[Fe^{2+}]_b$ = bulk concentration for Fe^{2+} (mol/m^3)
$[H^+]_b$ = bulk concentration for H^+ (mol/m^3)

The equations are of the following form,

$$F_i(x_j^*) = 0, \qquad i, j = 1 \rightarrow 3 \tag{14}$$

Taylor series expand about (x_j') ignoring the higher order terms,

$$F_i(x_j^*) = F_i(x_j') + \left.\frac{\partial F_i}{\partial x_j}\right|_{x_j'} (x^* - x_j') \tag{15}$$

Where,

x^* = final converged solution

x_j' = initial estimation

Combining Equation 14 and 15 and solving for ($x^* - x_j'$)= Δx_j

$$\left.\frac{\partial F_i}{\partial x_j}\right|_{x_j'} (\Delta x_j) = -F_i(x_j') \tag{16}$$

Hence, this set of three non-linear equations was linearized to the form

$$[J(i, j)](\Delta x_j) = - F_i(x_j') \tag{17}$$

Where [J(i, j)] is the Jacobian matrix whose (i, j)th element was obtained by taking partial derivative of F_i with respect to x_j (for i=1 to 3 and j = 1 to 3). The elements of the Jacobian matrix for the system of Equations 11, 12, and 13 are:

$$A(1,1) = K_{mt,Fe^{2+}} - 0.5K_{e,Fe^{2+}} \exp\left[\frac{F(x_3 - E^0_{Fe^{2+}} - \frac{RT}{2F}\ln(x_1))}{RT}\right] \tag{18}$$

$$A(1,2)=0 \tag{19}$$

$$A(1,3) = -K_{e,Fe^{2+}} x_1 \exp\left[\frac{F(x_3 - E^0_{Fe^{2+}} - \frac{RT}{2F}\ln(x_1))}{RT}\right]\frac{F}{RT} \tag{20}$$

$$A(2,1)=0 \tag{21}$$

$$A(2,2) = -K_{mt,H^+} - 4K_{e,H^+} \exp\left[\frac{-F(x_3 - E^0_{H^+} - \frac{RT}{2F}\ln(\frac{x_2^2}{H_2}))}{RT}\right] \tag{22}$$

$$A(2,3) = -2K_{H^+}x_2 \exp\left[\frac{-F\left(x_3 - E^0{}_{H^+} - \frac{RT}{2F}\ln\left(\frac{x_2{}^2}{H_2}\right)\right)}{RT}\right]\frac{-F}{RT} \tag{23}$$

$$A(3,1) = -0.5K_{e,Fe^{2+}} \exp\left[\frac{F\left(x_3 - E^0{}_{Fe^{2+}} - \frac{RT}{2F}\ln(x_1)\right)}{RT}\right] \tag{24}$$

$$A(3,2) = 2K_{e,H^+} \exp\left[\frac{-F\left(x_3 - E^0{}_{H^+} - \frac{RT}{2F}\ln\left(\frac{x_2{}^2}{H_2}\right)\right)}{RT}\right] \tag{25}$$

$$\begin{aligned} A(3,3) = {} & K_{e,H^+}x_2 \exp\left[\frac{-F\left(x_3 - E^0{}_{H^+} - \frac{RT}{2F}\ln\left(\frac{x_2{}^2}{H_2}\right)\right)}{RT}\right]\frac{-F}{RT} \\ & - K_{e,Fe^{2+}}x_1 \exp\left[\frac{F\left(x_3 - E^0{}_{Fe^{2+}} - \frac{RT}{2F}\ln(x_1)\right)}{RT}\right]\frac{F}{RT} \end{aligned} \tag{26}$$

The system of equations given by Equation 16 was solved by Gauss elimination method. Then the value of (x_j') was updated to (x_j' +Δx_j) and iterated again until the system of equations converged to the solution. In order to get started with Newton's method, initial estimations for three unknowns must be provided.

Corrosion Rate in Multiphase Slug Flow

The simplified CO_2 corrosion mechanistic model only predicts a corrosion rate in single phase flow. An extension to multiphase slug flow is needed. To calculate the overall corrosion rate in multiphase slug flow, the slug unit can be split into four separate components, slug film, slug mixing zone, slug body, and slug tail, as shown in Figure 2(a). If the characteristic information of slug film, slug mixing zone, slug body, and slug tail were known, the corrosion in each section can be calculated. Thereafter, Equations 27 and 28 can determine the overall corrosion rate.

$$C_R = C_{sf}(t_{sf}/t) + C_{sm}(t_{sm}/t) + C_{sb}(t_{sb}/t) + C_{st}(t_{st}/t) \tag{27}$$

$$t = t_{sf} + t_{sm} + t_{sb} + t_{st} \tag{28}$$

Where,

t = time for one slug (s)
t_{sf} = time for one slug film (s)
t_{sm} = time for one slug mixing zone (s)
t_{sb} = time for one slug body (s)
t_{st} = time for one slug tail (s)

However, the above method becomes too complex to use since the characteristic information of these four regions are not easy to obtain. The simplification of the above method becomes necessary and

practical. The previous mass tranfser experimenal study already approved that the peaks of the instantaneous mass transfer coefficient are directly caused by the bubble events in the stationary mixing zone.[29, 32] The stationary slug flow was specifically designed to produce a controlled mixing zone over a specific position in the pipeline for corrosion and inhibitor testing. It is found that the peak zone and base zone of the instantaneous mass transfer coefficients appear alternatively when slug mixing zone and slug film zone pass the electrode (Figure 3(a)). This is further shown in an enlarged Figure 3(b). Comparison of Figure 2 and Figure 3(b) clearly demonstrates the direct relationship between the peaks of the instantaneous mass transfer coefficient and the slug mixign zone. For example, the peak zone with five peaks of the instantaneous mass transfer coefficient from 9.8 to10.8 second correspond to one mixing zone in Figure 2, where gas bubble entrainment exists and five bubble collapsing were detected by the electrodes. On the contrary, the base instantaneous mass transfer coefficients from 10.8 to 11.6 second corresond to the slug film in Figure 2, where gas redistribution region,[27] slug body, and slug tail appears before another mixing zone. The instantaneous mass transfer coefficient between 9.8 and 11.6 second corresponds to a typical slug unit.

It is also noticed that the mixing zone does not always create multiple peaks of instantaneous mass transfer coefficient even in the same slug flow condition. Some slugs were well developed and produced a strong mixing zone where the bubbles can collapse on the wall in the form of pulses. Some slugs wre not well developed and thus no pulses of bubble collapsed on the wall. This has been confirmed by video.

Based on the above analyses, the corrosion modeling in slug flow can be simplified via the assumption that slug flow is composed of two distinctive regions: the mixing zone and the slug film, which is same as the method used in other models.[8, 10] The following calculation method can be obtained from Equation 27 and 28:

$$C_R = C_{sf}\,(t_{sf}/t) + C_{sm}(t_{sm}/t) \quad \text{or} \tag{29}$$

$$C_R = C_{sf}\,(1 - R_m) + C_{sm}\,R_m \tag{30}$$

$$t = t_{sf} + t_{sm} \tag{31}$$

$$R_m = t_{sm}/t \tag{32}$$

Where,

t_{sf} = time for one slug film (s)
t_{sm} = time for one slug mixing zone (s)
R_m = ratio of mixing zone time over one slug time
C_{sf} = corrosion rate in slug film (mm/yr)
C_{sm} = corrosion rate in slug mixing zone (mm/yr)

The new mass transfer correlations were developed recently for slug film and slug mixing zone, as shown in Equation 33 and 34,[33, 34] resepctively. They can be used in the above model to calculate the corrosion rates in slug film (C_{sf}) and slug mixing zone (C_{sm}), respectively. The applciation of these new mass transfer correlations distinguish this corrosion model from other models.[8, 10] The current simplification method becomes more reliable since the unique turbulence and mass transfer in multiphase slug flow were considered.

$$Sh = 0.544\,Re^{0.61}\,Sc^{0.33} \tag{33}$$

$$Sh = 0.00675\,Fr^{3.63}\,Re^{0.61}\,Sc^{0.33} \tag{34}$$

The calculations of the above used parameters are shown as follows:

Average slug time (s):

$$t = 1/f \tag{35}$$

$$\text{Log}\,(f \times D/V_{sl}) = m \times V_m + b \tag{36}$$

$$m = 4 \times 10^{-5}\theta^3 + 5 \times 10^{-4}\theta^2 - 2.5 \times 10^{-2}\theta + 0.7 \tag{37}$$

$$b = -4 \times 10^{-4}\theta^3 - 4.1 \times 10^{-3}\theta^2 + 2\theta - 1.7 \tag{38}$$

Where,

f = slug frequency (s^{-1})

D = pipeline diameter (m)

V_{sl} = superficial liquid velocity (m/s)

V_m = total gas/oil/water velocity (m/s)

θ = pipeline inclination (degree)

Average mixing zone time (s):

$$t_{sm} = LMZ/\ V_t \tag{39}$$

Average length of mixing zone = LMZ (m):

By correlation[27]

$$LMZ = 0.051\ Fr + 0.18 \tag{40}$$

or by mechanistic model[27]

$$LMZ = 1.5D + \frac{h_{ls} \times Fr_s \times \sqrt{gD}}{v_b} \tag{41}$$

$$v_b = 1.53\left[\frac{\sigma \times g \times \Delta\rho}{\rho^2}\right]^{1/4} \tag{42}$$

Where,

v_b = rise velocity of a moderate bubble calculated from equations (m/s)

h_{ls} = liquid height to gas/liquid interface (m)

v_m = mixture velocity with respect to pipe wall (m/s)

V_t = transitional mixing zone velocity (m/s) =1.25 (Vsl+ Vsg) (43)

V_{LF} = slug film Velocity (m/s) =Vsl[23] (44)

$$Fr_s = \text{slug Froude number} = \frac{v_t - v_m}{\sqrt{g \times D}} \tag{45}$$

$$Fr = \text{film Froude number} = \frac{V_t - V_{LF}}{\sqrt{(gh_{EF})}} \tag{46}$$

h_{EF} = effective film height obtained from the experiment measurement (m)

In a summary, the corrosion rate in multiphase horizontal slug flow can be calculated by the equations in the above three sections. This work presents a steady state corrosion mechanistic model without considering the transient variables. A transient corrosion mechanistic model for multiphase flow need much more efforts.[36]

RESULTS AND DISCUSSIONS

Water/Gas/Oil Multiphase Slug Low

Water/Gas Slug Flow. The mass transfer correlations Equations 33 and 34 were developed just for the slug film zone and the slug mixing zone, respectively.[33, 34] Therefore, these correlations were used to calculate the mass transfer coefficient in the CO_2 corrosion mechanistic model. The water physical properties were directly used in the calculations of Reynolds and Schmidt numbers in the water/gas two-phase slug flow.

Water/Gas/Oil Slug Flow. Zhang has suggested two methods to calculate the mass transfer coefficient for water/oil flow.[13] Both methods involved in situ water velocity and pipe diameter. In the first method mixture density and mixture viscosity, averaged on a volumetric basis, were used in the definitions of Reynolds and Schmidt numbers. In the second method, only the saltwater density and viscosity were used. The study of the in situ oil percentages in three-phase slug flow shows that the oil phase mixed very well with the water phase because of the enhanced turbulence induced by slug flow.[31] Therefore, water/oil mixture properties were used in the definition of Reynolds and Schmidt numbers in the liquid phase under water/gas/oil three-phase slug flow.

Corrosion computation was carried out for 40, 60, and 80 ºC in two phase and three phase slug flow under the pressure of 0.27 and 0.79 MPa. It is found in Table 2 that with the increase of oil percentage from zero to 20%, the corrosion rates decrease. For example, under the same pressure of 0.27 MPa, the two phase slug flow gives 8.8, 49.2, and 49.7 mm/yr corrosion rates under 40, 60, and 80 ºC, respectively while the corrosion rates in three phase slug flow decrease to 7.8, 36.2, and 35.6 mm/yr, respectively. It is shown that the predicted corrosion rate increases significantly with the increase of temperature at a high-pressure condition (Figure 5). However, at a low-pressure condition of 0.27 MPa, the temperature influence on the corrosion rates becomes negligible when temperature increases from 60 to 80ºC.

Comparison with Pots Model and Jepson Model

Comparison of three models, the Pots model, the Jepson model, and the current mechanistic model with the experimental corrosion data is shown in Figure 5. It indicates the Pots model underestimates the corrosion rates for slug flow since it neglects the bubble collapsing in the slug mixing zone. It seems that the current model overestimates the corrosion rates compared to the corrosion experimental data. The shear stress analysis indicated that the slug flow with high Froude number can remove the corrosion product layer.[34] Without the consideration of corrosion product film, this model predicts the maximum corrosion rate in slug flow. In addition, the peak mass transfer coefficient was assumed in the whole slug mixing zone. This might results into an overestimated ratio of the slug mixing zone time and one slug time, which becomes another reason to over predict the corrosion rates. The Jepson model was just developed from these laboratory experimental corrosion data as shown in Equation 47; therefore, it fits these data well.[14]

$$CR = 31.15 C_{oil} C_{freq} \left(\frac{\Delta P}{L}\right)^{0.3} \upsilon^{0.6} {P_{CO_2}}^{0.8} T \exp\left(\frac{-2671}{T}\right) \tag{47}$$

Gunaltun suggested that high accuracy in corrosion prediction is neither required nor possible because of the complexity involved in the production, corrosion control, and engineering design.[6] Only the "order of magnitude" of the corrosion rate has a practical meaning. The current mechanistic model gives a reasonable order of magnitude of the corrosion rate in slug flow. This becomes the major advantage for the current mechanistic corrosion model compared to the Jepson model and especially other models. An improvement of the new model could be achieved through a further investigation of two error resources: the ratio of the slug mixing zone time over one slug time shown in Equation 32 and the consideration of the corrosion product film.

Effect of Slug Flow on Corrosion Rate

Effect of Superficial Gas Velocity and Froude number. The calculation procedure of this mechanistic model is shown in Table 3. For example, at 60 ºC, 6 m/s superficial gas velocity, and 1 m/s superficial liquid velocity, the film Froude number 13.1 was first calculated based on the Equation 46. Then, the length of the slug mixing zone (LMZ) was obtained by Equations 40 or 41. The average mixing zone time (t_{sm}) of 0.097 was calculated by Equation 39. On the other hand, the average slug time (t) can be calculated from the slug frequency (f) in Equation 35. The ratio of the mixing zone time over the one slug time (R_m) was then obtained as 0.058 from Equation 32. The mechanistic model predicted a corrosion rate of 816.93 mm/yr in the mixing zone using the mass transfer correlation Equation 34. It gave a corrosion rate of only 1.75 mm/yr in the slug film using the mass transfer correlation Equation 33. The significant difference in the corrosion rate is a result of the enhanced mass transfer rate in the slug mixing zone. In the end, Equation 30 was applied to give the average corrosion rate (C_R) of 49.16 mm/yr in the slug flow.

Figure 6 directly presents the influence of superficial gas velocity on the corrosion rate in the slug flow. At a temperature of 40 ºC, the corrosion process is mass transfer controlled at low velocities (from 0 to 4 m/s or from Froude zero to 10.8), while it becomes reaction controlled at high velocities (above 4 m/s). The velocity of 4 m/s is named as the transitional velocity. This transitional velocity continues to go up with an increase in temperature since the reaction rate increases much more quickly compared to the mass transfer rate when the temperature increases. At a higher temperature, e.g. 60 or 80 ºC, the reaction speed increases significantly compared to 40 ºC. The reaction rate constants increase about 10 times, but the mass transfer coefficients increase only about 2 times. Therefore, the mass transfer controlled flow region extends to a superficial velocity of 6 m/s or higher. This shows that the effect of multiphase flow on corrosion is important, as is this study in general.

There is a close relationship between the Froude number and the superficial gas velocity as shown in Equation 46. Table 4 highlights that the Froude number dominantly influences the corrosion rate. For example, at 60 ºC when the Froude number increases from 6 to 10.8 and 13.1, the corrosion rate increases significantly from 4.80 to 32.19 and 49.16 mm/yr although the slug frequency decreases slightly. This trend is also observed at other temperatures.

Effect of Superficial Liquid Velocity and Slug Frequency. It is found that the superficial liquid velocity has an important impact on the corrosion rates (Figure 7). Under a low superficial liquid velocity (e.g. 1 m/s), the slug frequency is quite small, and the corrosion rate does not change much. However, a significant change in the slug frequency causes the corrosion rates to increase quickly when the superficial liquid velocity increases to 1.5 m/s. It is also noticed that the corrosion is reaction controlled under the temperature of 40 ºC. However, under a higher temperature, e.g. 60 or 80 ºC, and a

higher superficial liquid velocity (e.g. 1 m/s), the corrosion becomes mass transfer controlled because the reaction rate increases faster than the mass transfer rate.

Table 5 highlights the influence of slug frequency on the predicted corrosion rates at various superficial liquid velocities and at a 6.0 m/s superficial gas velocity in two phase slug flow under 0.27 MPa pressure. These three superficial liquid velocity conditions have similar Froude numbers, but differ in the slug frequency mainly influenced by the superficial liquid velocity as shown in Equation 36. The corrosion rate increases significantly with an increase in the slug frequency. For example, at 60 ºC, the predicted corrosion rate increases from 48.53 to 49.16 and 101.26 mm/yr when the slug frequency increases from 24 to 36 and 60 Hz. This changes is also clear at a higher temperature (e.g. 80 ºC).

CONCLUSIONS

1) A CO_2 corrosion mechanistic model is developed for the corrosion prediction of carbon steel pipeline under multiphase slug flow. The model considers chemistry, thermodynamics, enhanced solid-liquid mass transfer, and simplified electrochemical reaction kinetics. The slug flow was simplified into two regions: slug mixing zone and slug film zone. The special mass transfer correlations corresponding to these two regions were used in this model. No corrosion product film was assumed in the model since no film exists or only a thin film exists in most slug flows.

2) A comparison of the laboratory corrosion data and other models indicates that the CO_2 mechanistic model developed in this study is able to provide a reliable qualitative information on the corrosion rates in slug flow and the influence of multiphase slug flow on corrosion. An improvement of the new model could be achieved through a further investigation of two error resources: the ratio of the slug mixing zone time over one slug time and the consideration of the corrosion product film.

3) The superficial gas velocity is strongly associated with the dimensionless film Froude number of slug flow. This determines the dominant influence of the film Froude number on the corrosion rates. On the other hand, the clear influence of the slug frequency on the corrosion rates is also found. This provides an insight for the pipeline design and production.

ACKNOWLEDGMENTS

The authors would like to thank the permission to publish this paper from the advisory board companies of the Corrosion in Multiphase Systems Center. Also, a graduate fellowship from Texaco for Hongwei Wang is gratefully acknowledged.

REFERENCES

1. Nesic, S., Postlethwaite, J., Vrhovac, M., J. Corrosion Reviews, 15, (1997)
2. De Waard, C. and Williams, D. E., “Carbonic Acid Corrosion of Steel,” *Corrosion*, 31, 177 (1975)
3. De Waard, C., Lotz, U., and Milliams, D. E., “Predictive Model for CO_2 Corrosion Engineering in Wet Natural Gas Pipelines,” *Corrosion*, 47, 750 (1991)

4. De Waard, C., and Lotz, U., " Prediction of CO_2 Corrosion of Carbon Steel," Corrosion/1993, Paper No. 69, (Houston, TX: NACE International, 1993)

5. De Waard, C., Lotz, U., and Dugstad, A., " Influence of Liquid Flow Velocity on CO_2 corrosion: A Semi-empirical Model," Corrosion/1995, Paper No.128, (Houston, TX: NACE International, 1995)

6. Gunaltun, Y. M., "Combine Research and Field Data for Corrosion Rate Prediction," Corrosion/1996, Paper No. 27, (Houston, TX: NACE International, 1996)

7. Norwgian Technology Standards Institution, "CO_2 Corrosion Rate Calculation Model," NORSOK Standard No. M-506," http://www.nts.no/norsok, June 1998

8. Pots, B. F. M.," Mechanistic Models for the Prediction of CO_2 Corrosion Rates under Multiphase Flow Conditions," Corrosion/1995, Paper No. 137, (Houston, TX: NACE International, 1995)

9. Nyborg, R., Nordsveen, M., and Stangeland, A., "Kjeller Sweet Corrosion V, Final Report," Institute for Energy Technology, No. 75, (1998)

10. Nyborg, R., Anderson, P., and Nordsveen, M., " Implementation of CO_2 Corrosion Models in a Three-Phase Fluid Flow Model," Corrosion/2000, Paper No. 48 (Houston, TX: NACE International, 2000)

11. Jangama, V. R. and Srinivasan, S., "A Computer Model for Prediction of Corrosion of Carbon Steels," Corrosion/1997, Paper No. 318, (Houston, TX: NACE International, 1997)

12. Dayalan, E., Vani, G., Shadley, J. R., Shirazi, S. A., and Rybicki, E. F., "Modeling CO_2 Corrosion of Carbon Steels," Corrosion/1995, Paper No. 118, (Houston, TX: NACE International, 1995)

13. Zhang, R., Gopal, M., and Jepson, W. P., Development of a Mechanistic Model for Predicting Corrosion Rate in Multiphase Oil/Water Flows, Corrosion/1997, Paper No 601, (Houston, TX: NACE International, 1997)

14. Jepson, W. P., Stitzel, S., Kang, C., and Gopal, M., "Model for Sweet Corrosion in Horizontal Multiphase Slug Flow," Corrosion/1997, Paper No. 11, (Houston, TX: NACE International, 1997)

15. Adams, C.D., Garber, J.D. Singh R.K., "Computer Modeling to Predict Corrosion Rates in Gas Condensate Wells Containing CO_2," Corrosion/1996, Paper No: 31, (Houston, TX: NACE International, 1996)

16. High, M. S., Wagner, J., and Natarajan, S., "Mechanistic Modeling of Mass Transfer in the Laminar Sublayer in Downhole Systems," Corrosion/2000, Paper No. 62, (Houston, TX: NACE International, 2000)

17. Green, A.S., Johnson, B. V., and Choi, H., "Flow-related Corrosion in Large-Diameter Multiphase Flow Line," SPE, 20685, 677, (1990)

18. Sun, J. Y. and Jepson, W. P., "Slug Flow Characteristics and Their Effect on Corrosion Rates in horizontal Oil and Gas Pipelines," SPE 24787, (Washington, DC, 1992)

19. Chen, Y., Hong, T., and Jepson, W. P.,"EIS Studies of a Corrosion Inhibitor Behavior under Multiphase Flow Conditions," *Corros. Sci.,* 42, 979 (2000)

20. Gopal, M., Kaul, A. and Jepson, W. P., " Mechanisms Contributing to Enhanced Corrosion in Three Phase Slug Flow in Horizontal Pipes," Corrosion/1995, Paper No. 105, (Houston, TX: NACE International, 1995)

21. Jiang, L., Gopal, M., "Multiphase Flow-enhanced Corrosion Mechanisms in Horizontal Pipelines," *J. Energy Resour. Technol.,* 120, 67 (1998)

22. Wang, H., Cai, J. Y., Hong, T., and Jepson, W. P., "Current Oscillation of Oxidation of Ferrocyanide Anion in Two-Phase Slug Flow," 195th Meeting of The Electrochemical Society, Seattle, Washington, (1999)

23. Gopal M. "Visualization and Mathematical Modeling of Horizontal Multiphase Slug Flow, " Ph.D. Dissertation, Ohio University (1994)

24. Gopal, M. and Jepson, W. P., "Development of Digital Image Analysis Techniques for the Study of Velocity and Void Profiles in Slug Flow," *Int. J. Multiphase Flow*, 23, 945 (1997)

25. Gopal, M. and Jepson, W. P., "The Study of Dynamic Slug Flow Characteristics Using Digital Image Analysis – Part 1: Flow Visualization," *J. Energy Resour. Technol*., 120, 87 (1998a)

26. Gopal, M. and Jepson, W. P., "The Study of Dynamic Slug Flow Characteristics Using Digital Image Analysis – Part 2: Modeling Results," *J. Energy Resour. Technol*., 120, 92 (1998b)

27. Maley, L. C. and Jepson, W. P., "Liquid Holdup in Large-Diameter Horizontal Multiphase Pipeline," *J. Energy Resour. Technol.,* 120, 185 (1998)

28. Maley, L., Slug Flow Characteristics and Corrosion Rates in Inclined High Pressure Multiphase Flow Pipes, M.S. Thesis, Ohio University, 1997

29. Wang, H., Cai, J.Y., Hong, T., Gopal, M., Jepson, W. P., and Dewald, H. D., "Effect of Bubbles on Mass Transfer in Multiphase Flow," Corrosion/2000, Paper No. 50, (Houston, TX: NACE International, 2000)

30. Wang, H., Hong, T., Cai, J. Y., Dewald, H. D., and Jepson, W. P., "Enhancement of the Instantaneous Mass Transfer Coefficient in Large Diameter Pipeline under Water/Oil Flow," *J. Electrochem. Soc.*, 147, 2552 (2000)

31. Wang, H., Vedapuri, D., Cai, J. Y., Hong, T., and Jepson, W. P., "Mass Transfer Coefficient Measurement in Water/Oil Multiphase Flow, *J. Energy Resour. Technol*., 23, 144 (2001)

32. Wang, H., Wang, H.B., Jepson, W. P., and H. D. Dewald, "Enhancement effect of Gas Bubbles on Mass Transfer in Stationary Slug Flow," Submitted to *J. Solid-State Electrochem.*, (2001)

33. Wang, H., "CO_2 Corrosion Mechanistic Modeling in Horizontal Slug Flow," Ph.D. Dissertation, Ohio University, 2002

34. Wang, H., Cai, J. Y., Hong, T., Jepson, W. P., Bosch, C., "Enhanced Mass Transfer and Wall Shear Stress In Multiphase Slug Flow," Corrosion/2002, Paper No: 02501, (Houston, TX: NACE International, 2002)

35. Tanaka, N., Tamamushi, R., "Kinetic Parameters of Electrode Reactions," *Electrochim. Acta*, 9, 963 (1964)

36. Nesic, S., Nyborg, R., Stangeland, A., and Nordsveen, M., "Mechanistic Modeling for CO2 Corrosion with Protective Iron Carbonate Films," Corrosion/2001, Paper No: 01040, (Houston, TX: NACE International, 2001)

37. Bill Hedges, BP Corrosion, Inspection & Chemicals (CIC) Group, 2001

TABLE 1. COMPARISON OF CO_2 CORROSION PREDICTION MODELS FOR CARBON STEEL

Name	Year	Availability	Model Type	Flow consideration	Reference
De Waard et al.	1975-1995	Open	Semi-empirical model	Turbulent flow (single phase and multiphase)	De Waard et al. (1995) [2-5]
LIPUCOR Model	1979-1996	N/A	Empirical model	Gas line/wells, oil lines/wells	Gunaltun (1996) [6]
NORSOK M-506 model	1998	Open to public	Empirical model	Turbulent flow (single phase)	Norwgian Technology Standards Institution (1998) [7]
HYDROCOR Model	1995	N/A	Mechanistic model	Extend to slug flow	Pots (1995) [8]
KSC Model	1998	N/A, JIP* only	Mechanistic model, with scale formation	Turbulent flow	Nyborg et al. (1998) [9]
IFE Model	2000	N/A, JIP only	De Waard + NORSOK M-506	Extend to slug flow (Use OLGA Three-phase fluid flow model)	Nyborg et al. (2000) [10]
PREDICT Model	1996-2000	Demo, and JIP only	De Waard model	Multiphase flow	Jangama et al. (1996) [11]
Tulsa model	1995	N/A, JIP only	Mechanistic, no scale formation	Turbulent flow (single phase)	Dayalan et al. (1995) [12]
Ohio model	1995-2001	N/A, JIP only	Mechanistic and empirical, scale formation	Applied to multiphase flow	Zhang et al. (1998) [13] Jepson et al. (1997) [14]
USL model	1984-2000	N/A, Demo, JIP only	N/A	Gas-condensate wells	Garber et al. (1998) [15]
DREAM Model	1996-2000	N/A, JIP only	Mechanistic model, no scale formation	Down hole gas well	High et al. (2000) [16]
Cassandra Model	2001	N/A	Based on Pots model	Corrosion in multiphase flow	Bill Hedges [37]

*: JIP = Joint Industrial Participants

TABLE 2. USING THE DEVELOPED MASS TRANSFER CORRELATION TO PREDICT CORROSION RATES IN TWO-PHASE AND THREE-PHASE SLUG FLOW AT TEMPERATURE OF 40, 60, AND 80 ºC AND PRESSURE OF 0.27 AND 0.79 MPA

T (ºC)	CR (mm/yr)															
	Water/gas (Vsl=1 m/s, Vsg=6 m/s) Fr=13.1															
	Brine								20% Oil -80% Brine							
	0.27 (MPa)				0.79 (MPa)				0.27 (MPa)				0.79 (MPa)			
	Exp.	Mod.	Jepson	Pots	Exp.	Mod.	Jepson	Pots	Exp.	Mod.	Jepson	Pots	Exp.	Mod.	Jepson	Pots
40	10.6	8.8	8.7	1.5	13.3	11.9	20.4	2.1	7.8	7.8	8.1	1.1	11.2	11.3	19.1	3.1
60	18.4	49.2	15.4	2.0	37.8	92.1	36.3	5.8	17.0	36.2	14.4	1.4	34.4	85.4	33.9	4.1
80	24.6	49.7	25.7	1.9	58.5	143.3	60.6	5.3	22.0	35.6	24.0	1.3	53.2	102.4	56.7	3.8

TABLE 3. CALCULATION OF CORROSION RATE IN TWO-PHASE SLUG FLOW USING THE MECHANISTIC MODEL AT 0.27 MPA

Temp (°c)	Vsg (m/s)	Vsl (m/s)	Fr	LMZ (m)	T_{sm} (s)	f (1/s)	T (s)	R_m	Vt (m/s)	C_{sm} (mm/yr)	V_{lf} (m/s)	C_{sf} (mm/yr)	C_r (mm/yr)
40	6	0.5	14.4	0.914	0.113	24	2.500	0.045	8.125	128.69	0.5	0.88	6.63
60	6	0.5	14.4	0.914	0.113	24	2.500	0.045	8.125	1053.6	0.5	1.15	48.53
80	6	0.5	14.4	0.914	0.113	24	2.500	0.045	8.125	1103.6	0.5	1.05	50.68
40	6	1	13.1	0.848	0.097	36	1.667	0.058	8.75	128.95	1.0	1.34	8.76
60	6	1	13.1	0.848	0.097	36	1.667	0.058	8.75	816.93	1.0	1.75	49.16
80	6	1	13.1	0.848	0.097	36	1.667	0.058	8.75	827.82	1.0	1.61	49.66
40	6	1.5	14	0.894	0.095	60	1.000	0.095	9.375	128.78	1.5	1.71	13.83
60	6	1.5	14	0.894	0.095	60	1.000	0.095	9.375	1040.52	1.5	2.25	101.26
80	6	1.5	14	0.894	0.095	60	1.000	0.095	9.375	1087.84	1.5	2.06	105.60

TABLE 4. PREDICTED CORROSION AT VARIOUS SUPERFICIAL GAS VELOCITIES AND 1.0 M/S SUPERFICIAL LIQUID VELOCITY IN WATER/GAS SLUG FLOW AT 0.27 MPA

Vsg (m/s)	Froude	Slug frequency (Hz)	CR (mm/yr) at 0.27 MPa, water/gas slug flow, Vsl =1.0 m/s		
			Temperature (ºC)		
			40	60	80
0	-	-	0.45	0.75	1.02
2	6	46	3.64	4.80	4.42
4	10.8	44	12.33	32.19	30.69
6	13.1	36	8.76	49.16	49.66

TABLE 5. PREDICTED CORROSION AT VARIOUS SUPERFICIAL LIQUID VELOCITIES AND 6.0 M/S SUPERFICIAL GAS VELOCITY IN WATER/GAS SLUG FLOW AT 0.27 MPA

Vsl (m/s)	Froude	Slug frequency (Hz)	CR (mm/yr) at 0.27 MPa, water/gas slug flow, Vsg =6.0 m/s		
			Temperature (ºC)		
			40	60	80
0.5	14.4	24	6.63	48.53	50.68
1.0	13.1	36	8.76	49.16	49.66
1.5	14	60	13.83	101.26	105.60

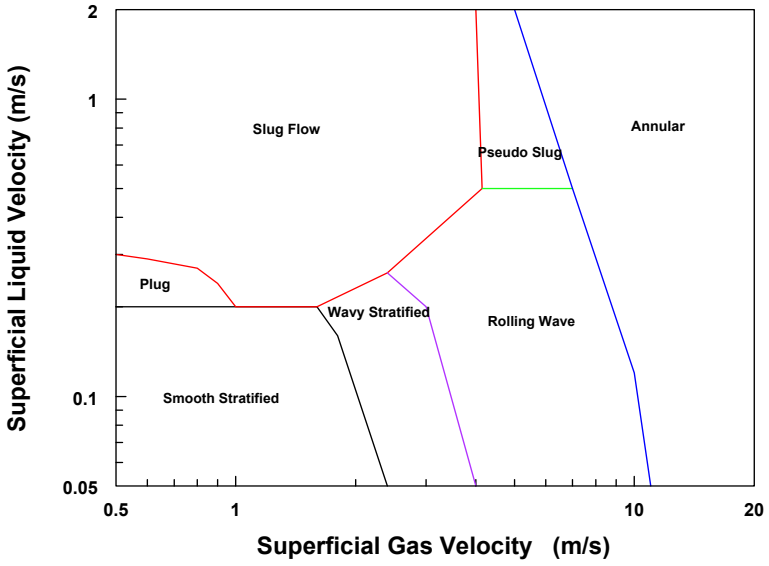

FIGURE 1 - A typical flow regime map for gas/oil/liquid three-phase flow in horizontal pipes (Lee, 1993)

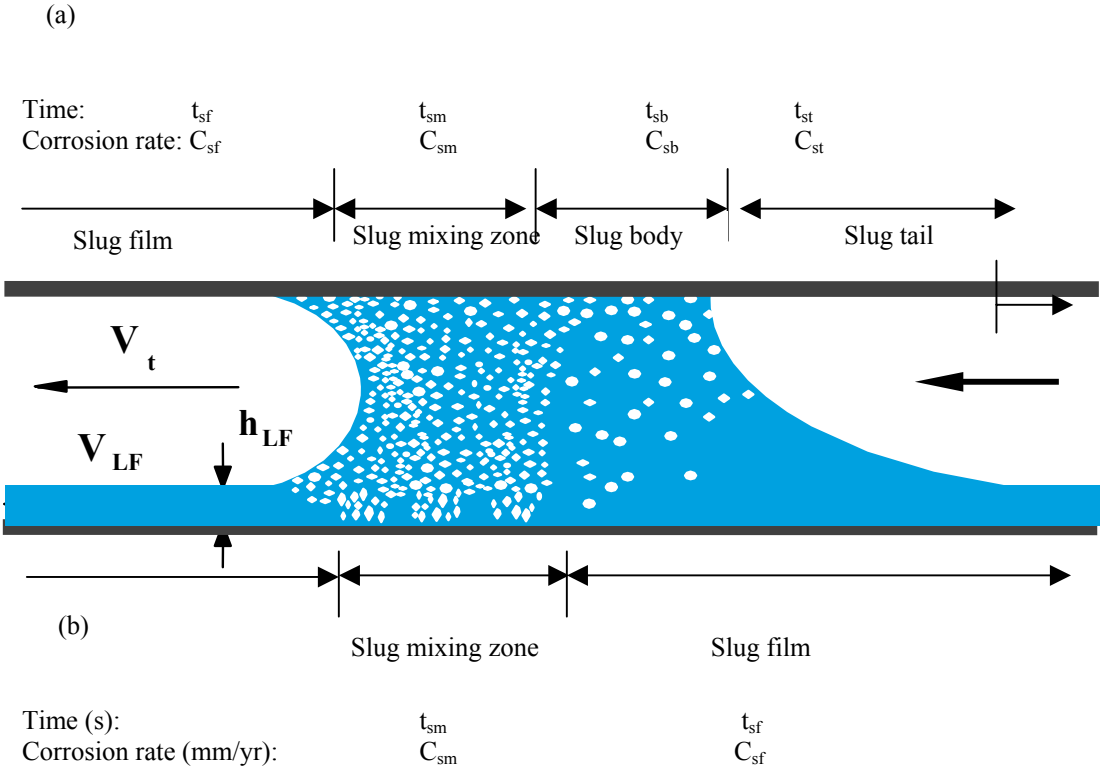

FIGURE 2 - Schematic of slug flow and calculation of overall corrosion rate by (a) four parts and (b) two parts in slug flow

(a)

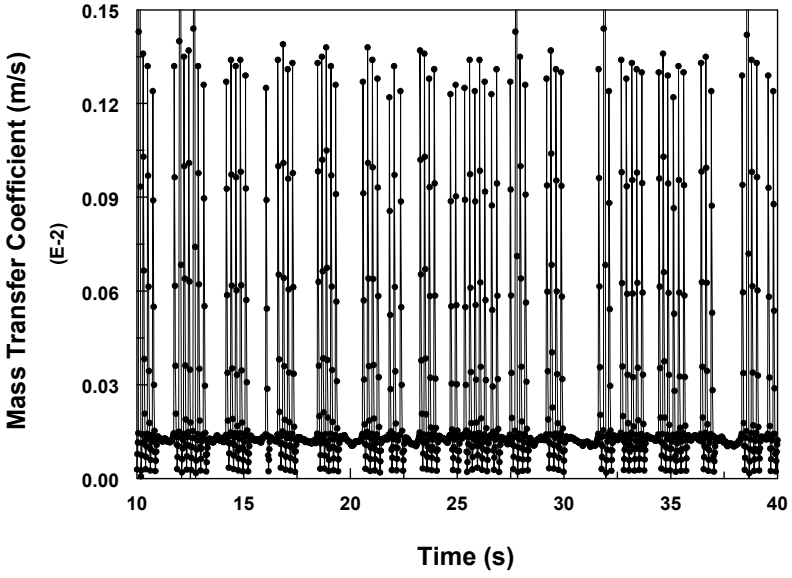

(b)

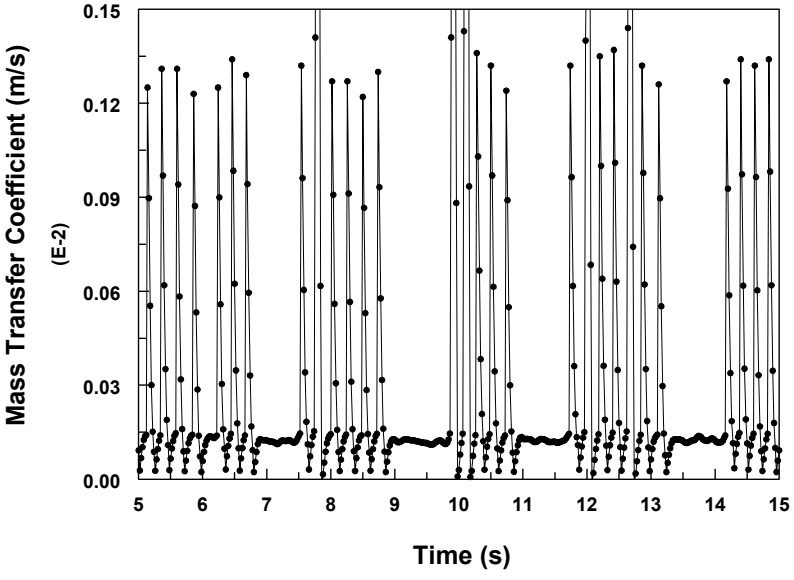

FIGURE 3 - Instantaneous mass transfer coefficient at Vsl=1.0 m/s and Vsg=1.4 m/s in water/oil/gas slug flow with 20% input oil (a) 10 – 40 s (b) 5 – 15 s

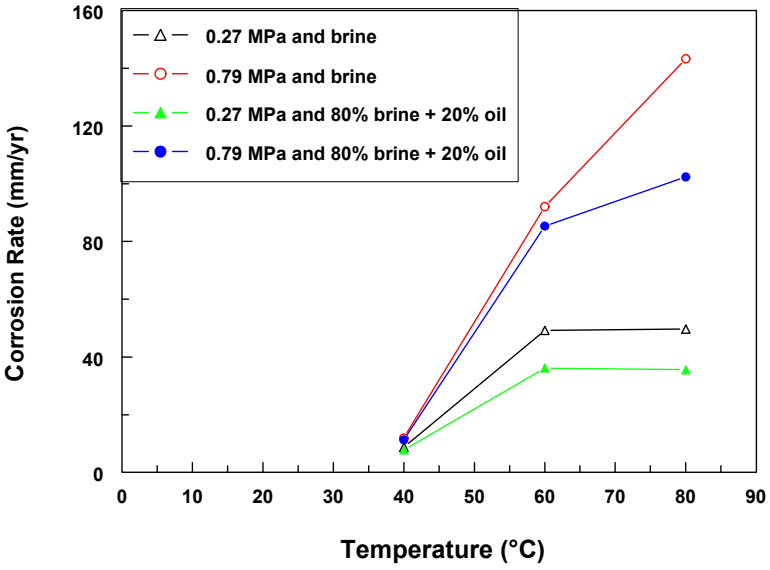

FIGURE 4 - Influence of temperature on corrosion rates in multiphase slug flow with Froude number 13.1

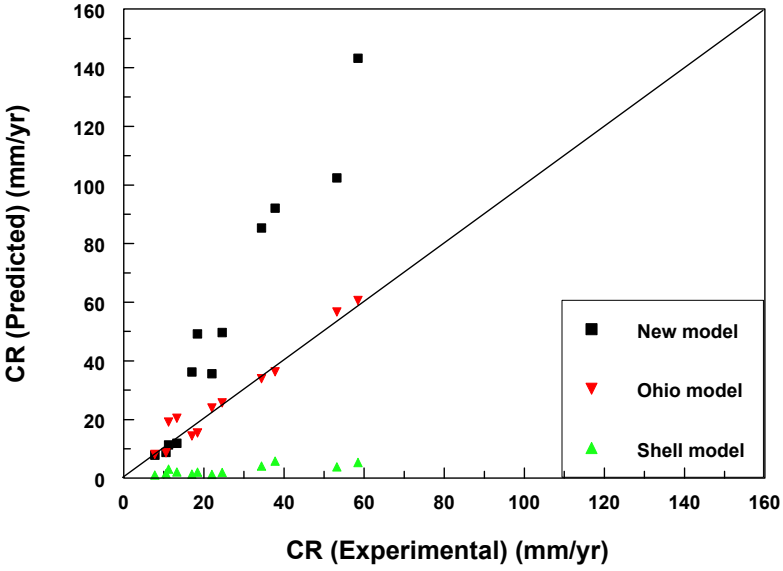

FIGURE 5 - Comparison of three corrosion models with experimental data

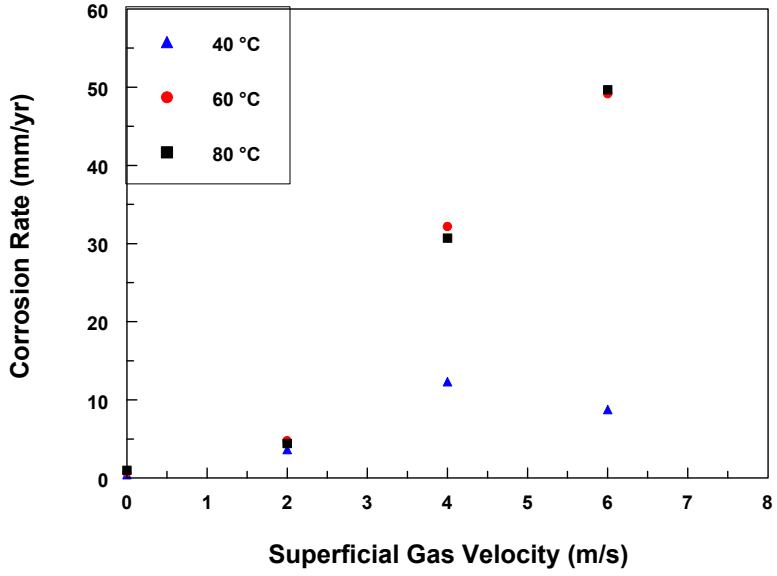

FIGURE 6 - Predicted corrosion rate vs. superficial gas velocity for 40, 60, and 80 ºC in ASTM seawater/gas slug flow at 0.27 MPa

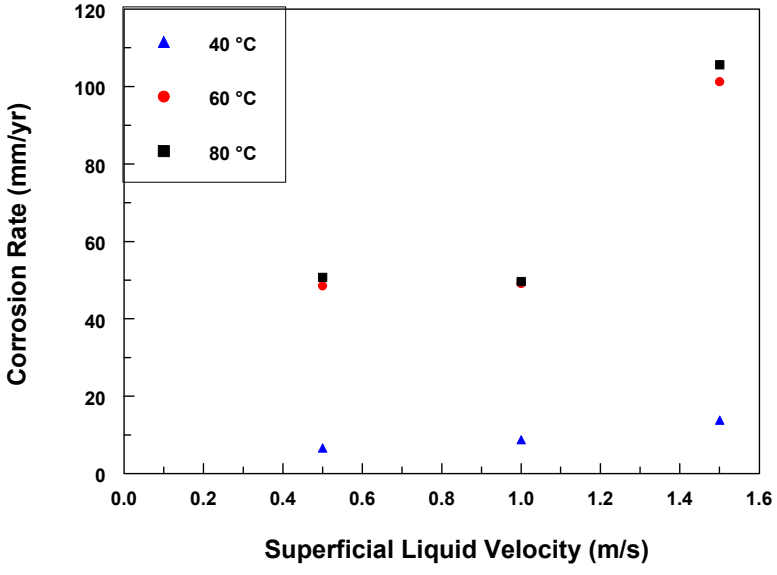

FIGURE 7 - Predicted corrosion rate vs. superficial liquid velocity for 40, 60, and 80 ºC in ASTM seawater/gas slug flow at 0.27 MPa